Current–Voltage Characteristics of High Current Density Silicon Esaki Diodes Grown by Molecular Beam Epitaxy and the Influence of Thermal Annealing

Michael W. Dashiell, Ralph T. Troeger, Sean L. Rommel, *Member, IEEE*, Thomas N. Adam, Paul R. Berger, *Senior Member, IEEE*, C. Guedj, James Kolodzey, *Senior Member, IEEE*, Alan C. Seabaugh, *Member, IEEE*, and R. Lake

***Abstract*—We present the characteristics of uniformly doped silicon Esaki tunnel diodes grown by low temperature molecular beam epitaxy ($T_{growth} = 275$ °C) using *in situ* boron and phosphorus doping. The effects of *ex situ* thermal annealing are presented for temperatures between 640 and 800 °C. A maximum peak to valley current ratio (PVCR) of 1.47 was obtained at the optimum annealing temperature of 680 °C for 1 min. Peak and valley (excess) currents decreased more than two orders of magnitude as annealing temperatures and times were increased with rates empirically determined to have thermal activation energies of 2.2 and 2.4 eV respectively. The decrease in current density is attributed to widening of the tunneling barrier due to the diffusion of phosphorus and boron. A peak current density of 47 kA/cm^2 (PVCR = 1.3) was achieved and is the highest reported current density for a Si-based Esaki diode (grown by either epitaxy or by alloying). The temperature dependence of the current voltage characteristics of a Si Esaki diode in the range from 4.2 to 325 K indicated that both the peak current and the excess current are dominated by quantum mechanical tunneling rather than by recombination. The temperature dependence of the peak and valley currents is due to the band gap dependence of the tunneling probability.**

***Index Terms*—Dopant diffusion, molecular beam epitaxy, negative differential resistance, rapid thermal annealing, silicon, tunnel diodes.**

Manuscript received December 1, 1999. This work was supported by DARPA under Contract F49620-96-C-0006, by ONR under Grant N00014-93-10393, and by ARO under Grants DAAH04-95-1-0625 and AASERT DAAG55-97-1-0249. The review of this paper was arranged by Editor K. O.

M. W. Dashiell, R. T. Troeger, S. L. Rommel, T. N. Adam, P. R. Berger, and J. Kolodzey are with the Department of Electrical and Computer Engineering, University of Delaware, Newark, DE 19716 USA (e-mail: dashiell@ee.udel.edu).

C. Guedj was with the Department of Electrical and Computer Engineering, University of Delaware, Newark, DE 19716 USA. He is now with the Paul Scherrer Institute, Villigen PSI, Switzerland CH-5232.

R. Lake is with the Applied Research Laboratory, Raytheon Systems Company, Dallas, TX 75243 USA.

A. C. Seabaugh was with the Applied Research Laboratory, Raytheon Systems Company, Dallas, TX 75243 USA. He is now with the Department of Electrical Engineering, University of Notre Dame, Notre Dame, IN 46556-5637 USA.

Publisher Item Identifier S 0018-9383(00)07380-9.

I. Introduction

TO ADDRESS issues of future device scaling and its limitations, researchers are focusing attention on new quantum devices, suitable for integration into silicon CMOS technology, with increased functionality, packing density and speed [1]–[5]. The negative differential resistance (NDR), bi-stability and high switching speeds associated with the quantum mechanical tunneling of electrons in devices including the Esaki tunnel diode, the resonant tunneling diode (RTD), and the resonant interband tunneling diode (RITD) may be exploitable for future logic, memory and oscillator circuits in computing and wireless communications applications.

Commercially available Si and Ge Esaki tunnel diodes are formed by alloying, a method incompatible with CMOS processing [5]. Few reports on a CMOS-compatible tunnel diode exist in the literature, such as Si and SiGe RITDs grown by molecular beam epitaxy (MBE) [6], [7], as well as p^+-i-n^+ diodes grown by MBE [8] and p^+-i-n^+ diodes combined with delta doping planes [9]. These diodes were grown at relatively low temperatures ranging from 325 to 370 °C. Two important figures of merits of tunnel diodes are the peak to valley current ratio (PVCR) and the peak current density. The highest PVCR for any epitaxially grown CMOS compatible tunnel diode is 4.2 (a $Si/Si_{0.5}Ge_{0.5}$ heterostructure Esaki with delta doping planes), while for an all Si diode it is 2.7 [9]. The addition of Ge to the intrinsic spacer was shown to increase the peak tunneling current as a result of lowering the tunneling barrier. The highest previously reported peak current density for a Si based tunnel diode was 22 kA/cm^2 for a $Si/Si_{0.5}Ge_{0.5}$ RITD grown at 370 °C [7]. For an all Si RITD of equivalent structure and growth conditions, the peak current density was approximately one order of magnitude less [7]. A high current density is important for high speed switching applications where fast charging is necessary.

An obstacle to achieving heavily doped n^+/p^+ epitaxial layers by any technique is the low solid solubility of many electrical impurities (dopants) commonly used for Si. During heavy doping of MBE films, a profound effect is the thermally activated surface accumulation of impurities occurring at conventional Si growth temperatures, resulting in low dopant incorporation and spreading of the dopant profile [10], [11]. Gossman *et al.* reported on a low temperature MBE (LTMBE)

(T_{growth} <300 °C) technique which results in crystalline Si layers with 100% electrical activation of Sb and B up to 6×10^{20} cm^{-3} and 1×10^{21} cm^{-3}, respectively, for layers grown below a critical thickness, $h_{epi}(T)$ [12], [13].

There are disadvantages, however, associated with low temperature growth. Jorke *et al.* observed a significant increase in bulk recombination currents due to mid-gap states for Si diodes grown at 325 °C compared to diodes grown at 500 °C [8]. Several authors have reported high concentrations of point defects [14] or microvoids [15], which were detected using positron annihilation spectroscopy. For example, Gossman *et al.* [14] found a density of vacancy-like defects of $\sim 10^{18}$ cm^{-3} for epitaxial Si films grown at 220 °C, while similar layers grown at 475 °C had a defect density of approximately three orders of magnitude less. However, these authors found that rapid thermal anneals (RTA) above 500 °C for 2 min reduced the defect density of the layers grown at 220 °C to below 5×10^{15} cm^{-3}, which is the sensitivity of the positron measurement.

In this paper, we present the properties of uniformly doped Si p$^+$-i-n$^+$ Esaki type diodes grown by LTMBE at 275 °C. We demonstrated a peak current density of 47 kA/cm^2 in a Si-only tunnel diode, which exceeds any previously reported Si based NDR device fabricated by epitaxy or alloying. We attribute our high current densities to the low growth temperature with high dopant incorporation. The PVCR of the diodes grown using this technique were slightly lower than reported in [8], [9], possibly a result of defects associated with the extremely high doping concentrations in our diodes. We quantitatively discuss the influence of post-growth annealing on the current–voltage (*I–V*) characteristics in the temperature range from 640–800 °C. The tunneling currents at constant biases were shown to decrease upon annealing with a rate characterized by thermal activation energies between 2.2–2.4 eV. *I–V* measurements taken between 4.2–325K revealed that the current is dominated by quantum mechanical tunneling for all applied voltage biases studied in this investigation.

II. Experimental

Uniformly doped Si Esaki diodes were grown by LTMBE in an EPI-620 MBE system. Si was evaporated from an electron gun at a rate of 0.5 nm/minute. P-type (boron) and n-type (phosphorus) dopants were evaporated from an elemental B source and a gettered compound GaP source [16], respectively. A 10-nm intrinsic Si spacer (i = nominally undoped) was grown between the n$^+$ and p$^+$ regions. The substrate temperature during growth was 275 °C, previously calibrated by observing the Au and Al eutetic reactions on a silicon substrate. A 15 nm p$^+$-type Si buffer ($N_A = 1 \times 10^{19}$ cm^{-3}) layer was grown on an 0.01 Ω-cm p-type (001) substrate, followed by the active regions: a 15 nm p^{++}-type Si layer, followed by a 10-nm i-layer, and finally the 30 nm n^{++}-type Si layer. Secondary ion mass spectrometry (SIMS) revealed peak P concentrations of $6 - 8 \times 10^{20}$ cm^{-3} and B concentrations of 4×10^{20} cm^{-3} in the active regions of the diode. The i-layer thickness was calculated from the Si growth rate and does not take into account the possibility of bulk or surface dopant segregation.

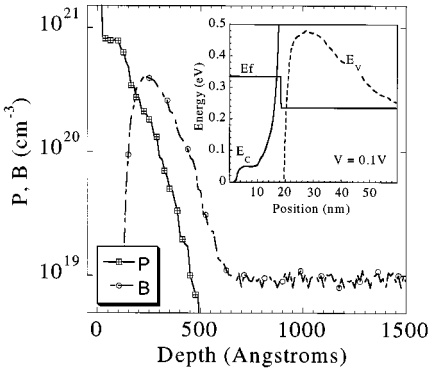

Fig. 1. SIMS profile of B and P dopants for the high current density Si p$^+$-i-n$^+$ Esaki diode prior to *ex situ* annealing. The inset displays the calculated band diagram where E_F is the quasi-Fermi level, E_C is the conduction bandedge and E_V is the valence bandedge.

The samples were annealed *ex situ* in an H_2/N_2 (15%/85%) ambient using a Heatpulse rapid thermal annealing (RTA) furnace. Mesa diodes 15 μm in diameter were formed using standard photolithography and aluminum metallization, followed by junction isolation by etching in a CF_4/O_2 plasma. Room temperature electrical characteristics were measured using a HP4156B semiconductor parameter analyzer.

Samples for low temperature measurements were fabricated using a 40×40 μm^2 square mesa with Ti/Au metallization. Bond pads were formed on top of a polyimide-insulating layer and were subsequently wire bonded into a package compatible with the cryostat. The cryogenic chamber was a Janis Research Inc., model number 14-CNDT Cryostat, and the temperature was controlled using a GaAs temperature sensor (1.4–330K) and a feedback controlled resistive heating element.

III. Results and Discussions

A. Current–Voltage versus Annealing

Fig. 1 displays the SIMS dopant profile for the Esaki diode prior to *ex situ* annealings. The SIMS profile reveals some deviation from the step type dopant profile expected from the growth conditions. It is possible, however, that this concentration spreading is an artifact of the SIMS measurement, since SIMS is known to suffer from knock-on and other effects which limit its depth resolution. Considering this uncertainty, it is difficult to exactly quantify the affects of dopant segregation, which may have occurred during growth. The inset of Fig. 1 displays the simulated band diagram near the junction under 0.1 V bias. The band diagram was calculated by self-consistently solving the effective-mass Schrödinger equation and Poisson equation for the charge profile taken from Fig. 1 (it was assumed that the dopants were completely activated), but does not consider effects such as band-tailing or states within the bandgap. As can be seen from the positions of the quasi-Fermi levels relative to their respective band-edges, the doped layers are highly degenerate with a tunneling barrier width of approximately 4–5 nm.

Fig. 2 displays the room temperature current density versus applied voltage characteristics (J–V) of the Si Esaki diode discussed above, after selected *ex situ* RTA anneals. The left-hand graph shows the J–V characteristics of the diode after 60 s

isochronal RTA anneals. The right hand side shows the J–V characteristics after isothermal annealing at 775 °C. Negative differential resistance is observed for the lower three annealing temperatures (Fig. 2, left) and for the shortest two anneal times (Fig. 2, right). Due to the high current density, unannealed samples burned out before any NDR was observed, even under pulsed measurements. Table I lists the peak and valley current densities and their PVCR. Because of the high current the series resistance in the measurement setup (approximately 6 Ω for unpackaged diodes) shifts the peak and valley currents to higher voltages. Analysis in the remainder of this section corrects the J–V data by removing this IR drop.

The diode currents in Fig. 2 are several orders of magnitude higher than expected from normal diode diffusion current. Jorke observed large deviations from ideal diode current in MBE grown p^+-i-n^+ Si diodes in the same bias range, for i-layer thicknesses of 40 nm and less [8]. They observed negative differential resistance for i-layers of 10 nm and 5 nm. These observations are consistent with earlier studies of alloyed junction Si Esaki diodes [17]–[19], where the current transport below the onset of NDR was shown to be due to phonon assisted tunneling transitions from conduction to valence band states (the band to band tunnel current). The current at, and beyond, the valley voltage, referred to as the excess current, was shown to be due to tunneling through defect levels in the forbidden energy gap up to a voltage where the thermal (i.e., diffusion or recombination) current begins to dominate. Both the band-to-band tunnel current and the excess current are proportional to an effective density of states and the probability for a tunneling transition to occur. The effective density of states for band-to-band tunneling can be expressed as an overlap integral between the density of states in the valence and conduction band multiplied by the occupational probabilities at a given energy [20]. Studies of the effects of high energy electron bombardment on the excess current on Si and Ge Esaki diodes revealed that the excess current increased proportionally to the electron dose [19]. The bombarding electron energy introduced defect energy levels within the material bandgap. Thus, the magnitude of the excess current was proportional to the density of defect states within the gap. The tunneling probability for both the band to band at constant bias and excess tunneling currents are exponentially dependent on effective mass, the barrier height and width, and field strength [20], [21]. Expressions for the band to band tunneling current (J) and the excess tunneling current (J_x) are, respectively, as follows:

$$J = Const \times D \times \exp\{-\beta m^{*1/2} n^{*-1/2} E_G\} \quad (1)$$

$$J_x = Const \times D_x \times \exp\{-(\alpha_x n*^{-1/2}\, e^{1/2}) \cdot (E_G - eV + 0.6(V_n + V_p))\}. \quad (2)$$

The density of defect states is given by D_x, α_x is a material constant, e is the elementary charge, n^* is the effective carrier concentration, E_G is the band gap, V_n and V_p are the quasifermi levels in the conduction and valence bands in volts, and V is the externally applied bias voltage across the junction. Equation (1) is a simplified expression for the band to band tunneling current using the abrupt junction approximation and assuming the junction potential is approximately equal to the bandgap voltage

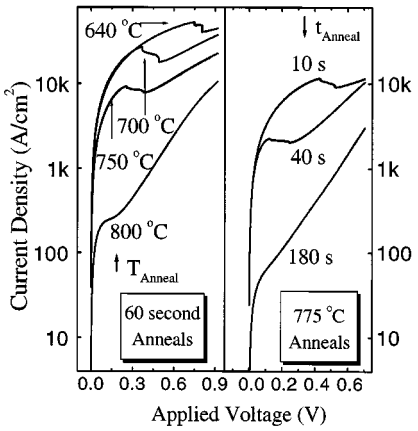

Fig. 2. Current density versus the applied voltage for a LTMBE Si tunnel diode after 60 s anneals at various temperatures (left hand plot). The right hand plot displays the same diode structure after annealing at 775 °C for various times.

[21]. The parameters β and m^* (tunneling effective mass) are constants and D represents the density of states overlap integral at a given bias (β is bias dependent).

For the abrupt junction approximation, the zero bias depletion width (W_0) is inversely proportional to the square root of the effective carrier concentration n^*, defined by

$$\frac{1}{n^*} = \left(\frac{1}{n} + \frac{1}{p}\right) \sim W_0^2 \quad (3)$$

where n and p are the electron and hole concentrations on either side of the junction. Because $n^{*-1/2}$ is proportional to the depletion width, it is referred to as the junction width parameter. The band to band tunnel current and the peak current depend exponentially on $n^{*-1/2}$ [18]. This is a consequence of the exponential dependence of the tunneling probability on the width of the tunneling barrier, i.e., the depletion region.

We determined the effective values of n^* versus annealing temperature for our high current density p^+-i-n^+ Si tunnel diodes by extrapolating the straight-line fit of $\ln(J_{25\ \mathrm{mV}})$ versus $n^{*-1/2}$ in [18, Fig. 2] to our $J_{25\ \mathrm{mV}}$ values (corrected for series resistance). The bias of 25 mV is chosen to be consistent with Logan's data [18], and because at this bias the current transport is expected to be solely due to tunneling between conduction to valence band states; the contribution from the excess or defect current becomes significant only at higher biases. From the results in Table I we note that the effective value of n^* decreases as a function of anneal temperature.

Fig. 3 depicts the natural logarithm of the current density (corrected for series resistance) at 25 mV (closed triangles) and 350 mV (open triangles) versus $1/k_B T_{anneal}$ for 1-min post growth anneals, where k_B is Boltzmann's constant. The inset of Fig. 3 shows the decrease in current density at 25 mV and 350 mV versus isothermal (775°C) annealing time. An empirical expression for the tunneling current at constant bias is

$$J = J_o \exp(-r t_{anneal}) \quad (4)$$

with a thermally activated rate r

$$r = r_o \exp(-E_A/k_B T_{anneal}) \quad (5)$$

where J_o and r_o are constants, and t_{anneal} and T_{anneal} are the annealing times and temperatures, respectively.

Fitting the data in Fig. 3 to equations (4) and (5) (solid lines) gives values for the activation energy $E_A = 2.24 \pm 0.42$ eV for the current at 350 mV, and $E_A = 2.39 \pm 0.36$ eV for the current at 25 mV. As discussed previously, the current at 25 mV bias is assumed to be dominated by band-to-band tunneling. We assume also that at 350 mV the excess current is due to tunneling through defect levels as in [19]. The latter assumption is further validated in the following section where the current at a constant bias of 325 mV was shown by its temperature dependence to be a tunneling current. From the extracted activation energies and their uncertainties, it is apparent that both tunneling currents (band to band and defect related tunneling current) have nearly the same dependence on thermal annealing. This explains why the PVCR only varies by a factor of 1.5, while the absolute magnitudes of peak and valley currents vary by more than two orders of magnitude over the range of annealing temperatures. We note from (1) and (2) that the one common variable for both the band-to-band current and the excess current is the exponential dependence on the tunnel barrier width [via $n*$ in equations (1) and (2)]. As discussed in more detail below, we conclude that for the annealing conditions used in this study, the change in magnitudes of the peak and valley currents are due to broadening of the tunnel barrier which occurs for anneals above 640 °C.

Duschl *et al.* has recently reported on the dependence of the peak and valley current on one minute anneals in the temperature range from 550 to 750 °C for heterostructure/delta doped Si/$Si_{0.5}Ge_{0.5}$ p^+-i-n^+ tunnel diodes [9]. These authors observed two trends in the post annealing *J–V* characteristics, where we distinguish between the low temperature (<680 °C) and high temperature (>680 °C) behavior. As the annealing temperature was increased from 550 to 680 °C, the peak current of the Si/$Si_{0.5}Ge_{0.5}$ tunnel diode remained essentially constant, while the valley current decreased. In this temperature region, the PVCR increased from approximately 1 to the maximum value of 4.2 for a 680 °C anneal. These authors attributed this behavior to the annealing of electrical active point defects, which were formed during low temperature growth. A reduction in the number of these defects will decrease the density of defect states [D_X in (2)]. Justification of their conclusion may be found in [14] where the density of vacancy-like defects in Si epitaxial layers grown by LTMBE was reduced by three orders of magnitude after annealing above 500 °C [14]. However, no activation energy was reported for either study. Previous authors have correlated the annealing dependence of excess currents in alloyed junction Si Esaki diodes with a decrease in point defects. Logan *et al.* [23] examined the effect of electron induced damage to the lattice on the excess current and the effects of post-bombardment annealing. Annealing at temperatures from 300–400 °C reduced the excess current to its pre-bombardment magnitude at a rate characterized by an activation energy of 1.3 eV. The increase/decrease in excess current was attributed to the creation/annihilation of defect states within the bandgap [i.e., an increase/decrease of D_X in equation (2)]. During these electron irradiation/annealing experiments, the peak current remained nearly constant, indicating that the width of the tunnel barrier was essentially unaffected during irradiation/bombardment.

TABLE I
ANNEALING DEPENDENCE OF SI ESAKI DIODE ELECTRICAL PROPERTIES FOR ONE MINUTE ANNEALS. THE VALUES WERE AVERAGED FOR FIVE DIODES AND THE STANDARD DEVIATION IS GIVEN. THE VALUES OF THE REDUCED CARRIER CONCENTRATION, n^* WERE EXTRAPOLATED FROM THE DATA GIVEN IN [18]. * THE DIODE ANNEALED AT 800°C DID NOT EXHIBIT NEGATIVE DIFFERENTIAL RESISTANCE

Anneal Temperature °C	J_{peak} (kA/cm^2)	J_{valley} (kA/cm^2)	PVCR	Extrapolated n^* ($\times 10^{19}$ cm^{-3})
640	46.8 ± 3.1	35.8 ± 1.0	1.3 ± 0.06	4.9
680	43.4 ± 1.9	29.2 ± 1.3	1.47 ± 0.05	4.8
700	26.1 ± 0.7	18.4 ± 1.3	1.425 ± 0.06	4.4
720	19.0 ± 1.9	14.1 ± 1.2	1.34 ± 0.04	4.0
750	9.3 ± 0.2	7.9 ± 0.09	1.17 ± 0.01	3.7
775	3.6 ± .05	3.2 ± 0.06	1.1 ± 0.01	3.5
800	0.05*	-	-	2.2

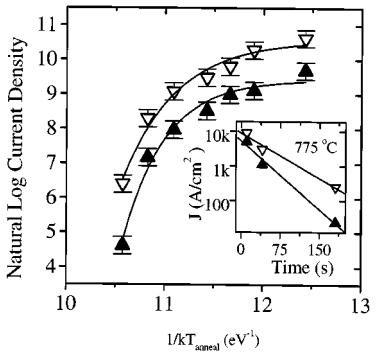

Fig. 3. Natural logarithm of current density versus the inverse of the annealing temperature (T_{ann}) at constant biases and for 60 s anneals, where k_B is the Boltzmann factor. The open triangles represent the current at 350 mV, while the filled triangles represents the current at 25 mV after series resistance corrections. The data was fit to equations (4) and (5), giving an activation energy of 2.24 eV ± 0.42 eV and 2.39 ± 0.36 eV. The inset to Fig. 2 shows the decrease in current as a function of isothermal annealing time.

For annealing temperatures of 680 °C and above (the high temperature region), Duschl *et al.* found that the peak and valley currents decreased at the same rates and more rapidly than for the low temperature anneals [9]. They attributed the decrease to a broadening of the depletion zone due to smearing of both the B and P delta doping spikes, which was confirmed by SIMS.

The high current density Si Esaki diodes that we investigated in this article were annealed under conditions similar to the high temperature anneal region in [9]. From the nearly equivalent thermal dependencies of the band-to-band and the excess currents, we concluded that the dominant mechanism occurring during *ex situ* annealing was the broadening of the tunnel barrier width, which is consistent with Duschl's conclusions for their P and B doped tunnel diodes. For our uniformly doped p^+-i-n^+ Si Esaki diodes, we expect that the broadening of the tunneling barrier is due to dopant diffusion from the heavily doped p^+ and n^+ layers into the intrinsic spacer layer. Using the abrupt junction approximation, we calculated the relative changes in the tunnel barrier width in terms of the extrapolated n* values

listed in Table I. We then approximated a characteristic redistribution length of P and B into the intrinsic spacer using the diffusion data for P and B given in [24] and the solution of the diffusion equation for a pair of semi-infinite solids [25]. For all annealing conditions, the change in the tunnel barrier width determined from the extrapolated $n*$ values were in reasonably good agreement with those values calculated for the characteristic redistribution length of the P and B dopants. Based on the decrease in the 25 mV tunneling current from the value at 640 °C to that after 1 min annealing at 680 °C (800 °C), the values of $n*$ in Table I correlated to an increase of 2 Å (25 Å) in barrier width respectively. Calculations for the relative redistribution lengths for both P and B summed together are ~2 Å (20 Å) for one minute anneals at 680 °C (800 °C).

The origin of the activation energy empirically determined from Fig. 3, may now be correlated with the diffusion of dopants from the n^{++} and p^{++} active regions into the intrinsic spacer layer. From the preceding paragraph, the dependence of the depletion width on the annealing conditions may be given by

$$W = W_{oi}\left(1 + \Theta\sqrt{Dt}\right) \tag{6}$$

where

W_{oi}	initial depletion width before annealing;
t	anneal time;
D	thermally activated diffusion coefficient for dopant redistribution;
$D = D_o \exp(-\Delta/k_BT)$	($D_o$constant and Δ effective activation energy for dopant diffusion);
$(Dt)^{1/2}$	characteristic re-distribution length;
Θ	constant of order unity.

Since tunneling current is exponentially dependent on the width of the tunneling barrier, we derive an expression for the temperature dependence of the tunneling barrier from equation (6) as follows:

$$J(T) = J_{oo}\exp\left\{-\gamma\sqrt{D_o t}e^{-(\Delta/2k_BT)}\right\} \tag{7}$$

where γ is a constant. Comparing (7) to (4) and (5) to determine the empirical activation energies for the rate of decay of the tunneling current, we see that our empirical activation energy corresponds to a value of $\Delta \sim 4.4-4.6$ eV. For high impurity concentrations, the diffusivity of a dopant in Si is most accurately described by a sum of the various impurity-vacancy interaction components, each with its own activation energy and concentration dependent pre-factors [26]. For most group III and IV elements in Si, these activation energies are between 3.5 and 4.5 eV. We note that the activation energy given in [26], which is close to our empirically determined value of −4.5 eV, is for the diffusion of P via a doubly ionized acceptor type vacancy with Δ =4.37 eV.

The optimal anneal temperature for high PVCR in our study, as well as that in reference [9], is 680 °C. This temperature should correspond to that where defect annealing is most rapid, however; it is still low enough to prevent dopant redistribution from increasing the barrier width; thus the peak current remains essentially constant. The use of dopants with lower diffusivities, such as Sb and As, may permit higher temperature stability of the peak current and possibly greater PVCR since their diffusion coefficients are lower than for B and P in Si [22]. A low bulk diffusivity will allow anneals at higher temperatures and times so that defect annealing is maximized (excess current reduced), yet the tunnel barrier will remain unchanged (peak current remains constant). Silicon RITD structures synthesized using Sb and B delta doping planes indicate that Sb does not diffuse for one minute anneals at 700 °C, while the B significantly redistributes itself [27].

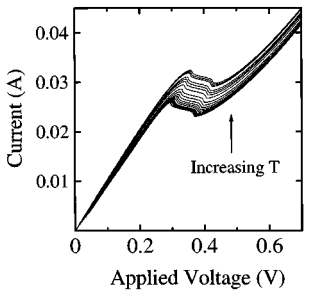

Fig. 4. Variable temperature *I–V* curves of a 40×40 μm^2 Si Esaki tunnel diode after a 60 s anneal at 775 °C. Measurement temperatures ranged from 4.2 to 325 °K. The variation of peak voltage versus peak current yields a series resistance of 8 Ω.

B. Current–Voltage Characteristics from 4.2 to 325 °K

The previous section suggested that both the peak and the excess currents were due to quantum mechanical tunneling. These assumptions were consistent with previous studies of alloyed junction Si Esaki diodes. Since MBE is a nonequilibrium growth process, the impurities and other defects may exist in concentrations significantly higher than by equilibrium growth methods and consequently can lead to high excess current. To verify the tunneling nature of the low bias (band to band) and high bias (excess) currents, we measured their dependence on diode operating temperature. The *I–V* characteristics after annealing in forming gas 775 °C (60 s) were measured as described in the experimental section. Fig. 4 shows the current voltage curves of the Si Esaki diode at measurement temperatures from 4.2 to 325 K. As the temperature increased, a variation of less than one order of magnitude in current was observed. A series resistance of 8 Ω in this measurement setup accounts for the increase in peak voltage as the peak current is increased. A weak temperature dependence of the current is typical for tunneling, which is not thermally activated in contrast to the normal diode diffusion or recombination current. Fig. 5 plots the PVCR versus measurement temperature (left axis) and the ratios of the peak, valley and constant bias (325 mV) currents to their respective 4.2 K current magnitudes. It is evident that the peak and valley currents exhibit almost exactly the same temperature dependence up to about room temperature. The excess current at constant bias (325 mV-corrected for series resistance) likewise exhibits a weak temperature dependence.

The ratio of the peak tunneling current to its value at 4.2 K can be derived from (1) in the previous section

$$\frac{I_{tunnel}(T)}{I_{tunnel}(4.2°\mathrm{K})} = \exp[-\beta m^{*1/2} n^{*-1/2}\Delta E_G]. \tag{8}$$

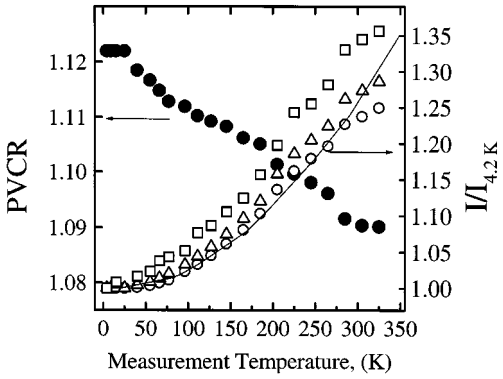

Fig. 5. Peak-to-valley current ratio (PVCR) of the diode from Fig. 4 as a function of measurement temperature (filled circles, left axis). The right axis shows the correct scale for the ratio of the peak (open circles) and valley (open triangles) currents as well as the current at a constant bias of 325 mV (open squares) normalized to their respective current values at 4.2 K. The solid line is a fit to (8) using the optical bandgap data of reference [24], illustrating that the temperature dependence of the tunneling current is due to the change in bandgap in the tunneling probability.

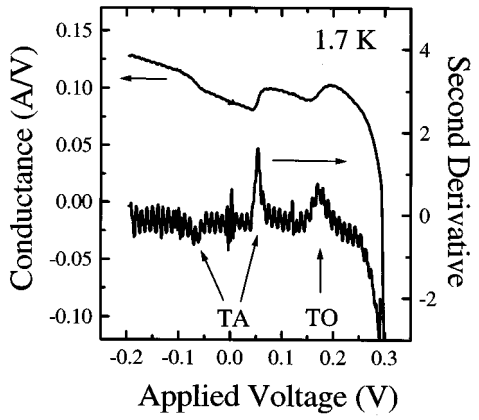

Fig. 6. Conductance, dI/dV (left axis) and the second derivative, d^2I/dV^2 (right axis) of the LTMBE grown Si Esaki diode from Fig. 4 taken at 1.7K. After correcting for series resistance, we attribute the inflections to contributions from the TA (18.4 meV) and TO (57.6 meV) phonons to the tunneling current.

We have fit the temperature dependence of the peak current ratios to the above equation using the optical bandgap temperature dependence data of [28] to obtain the solid line shown in Fig. 5. A value of 5.1 eV^{-1} is obtained for $\beta m^{*1/2} n^{*-1/2}$. The good fit between the experimental curves of $I_{peak}(T)/I_{peak}$(4.2 K) and equation (8) illustrate that the temperature dependence of the tunneling currents is due to the tunneling transition probability expression, where the change in bandgap (ΔE_G) is the only temperature dependent term.

The valley and the excess currents at a constant bias of 325 mV (corrected for series resistance) likewise follow an exponential dependence on Si bandgap up to around room temperature, implying the tunneling nature of the excess current. In Fig. 5, the slight deviation of the normalized valley current and current at 325 mV from the calculated curve for the peak current may be explained by the fact that the factor β in equation (8) actually depends on bias through the field strength at the junction. Thus, over the temperature and bias conditions we have studied, we rule out recombination currents inside the depletion region or at the surface as contributors to the excess currents because these currents exhibit strong thermal dependencies.

To observe the fine structure of the *I–V* characteristics, we have submerged the sample in liquid helium and evacuated the submersion chamber to achieve a measurement temperature of 1.7 K. An observable increase in the conductance at energies corresponding to certain phonon (or combination of phonons) energies is expected in an indirect material such as Si due to momentum conservation [17]. Fig. 6 shows the first and second derivatives of the *I–V* characteristics at biases from −200 mV to +300 mV. Three inflections are evident in the first derivative curve and become more pronounced in the second derivative curve where the phonon energy is approximately indicated by the maximum of the second derivative peak [17]. For the diode shown in Fig. 4, these values occur at −66, +53 and +173 mV. A correction of 8 Ω for the series resistance of the unpackaged diode give values of −17, +18 and +49 mV. These values are reasonably close to the values assigned by Chynoweth for the transverse acoustic (18.4 meV) and the transverse optical (57.6 meV) phonon branches and indicate that phononassisted tunneling is the dominant band-to-band tunneling mechanism for Si Esaki diodes grown by LTMBE.

IV. Conclusions

We have presented *I–V* results and the effects of post growth rapid thermal annealing on uniformly doped Si Esaki diodes grown by MBE. We have shown that all tunneling currents are reduced by annealing for one minute between 640 and 800 °C. The decrease in tunneling currents is attributed to an increase of the tunnel barrier due to dopant redistribution. The rate of current decrease was empirically characterized by a an activation energy of between 2.2 and 2.4 eV, and we developed a simple model relating these values to the activation energy for dopant diffusion. An optimal annealing temperature of approximately 680 °C for maximal PVCR in Si Esaki diodes doped with P and B appears to occur at the transition temperature where the mechanism dominating the *I–V* characteristics changes from defect annealing to dopant redistribution. An optimal annealing temperature is expected when comparing the activation energy for spreading of the tunnel barrier to the lower activation energy (1.3 eV) characterizing the annealing of point defects in Si Esaki diodes [23]. These conclusions suggest that higher PVCR may be obtainable by using dopants with lower diffusivities such as As and Sb, since higher temperatures may be used for point defect annealing (decreasing valley current), while maintaining the original doping profile (maintaining peak current).

Variable temperature *I–V* measurements were used to verify that both the peak current and excess currents were dominated by tunneling currents rather than thermally activated recombination or diffusion currents. Inflections in the diode conductance were observed at cyrogenic temperatures, consistent with phonon assisted tunneling in an indirect band gap semiconductor. The measured peak current density of 47 kA/cm^2 is higher than that reported for any Si based tunnel diode grown by MBE or formed using the alloy process.

ACKNOWLEDGMENT

The authors thank R. G. Wilson for SIMS measurements, M. Green for processing assistance, and P. Thompson and K. Hobart of the Naval Research Laboratory for discussions concerning MBE growth; B. Aldert of Raytheon Systems for invaluable assistance with the low temperature measurements; and M. Mauk, P. Sims, B. Feyock, and J. Cox of AstroPower Inc. for assistance with plasma etching and the polyimide process.

REFERENCES

[1] A. Seabaugh, R. Lake, B. Brar, R. Wallace, and G. Wilk, "Beyond the roadmap technology: Silicon heterojunctions, optoelectronics and quantum devices," in *Proc. Materials Research Soc. Symp.*, vol. 486, 1998, pp. 67–77.

[2] J. P. A. van der Wagt, "Tunneling based SRAM," *Proc. IEEE*, vol. 87, pp. 571–595, 1999.

[3] R. H. Mathews *et al.*, "A new RTD FET logic family," *Proc. IEEE*, vol. 87, pp. 596–605, 1999.

[4] P. Mazumber *et al.*, "Digital circuit applications of resonant tunneling devices," *Proc. IEEE*, vol. 86, pp. 664–686, 1998.

[5] A. Seabaugh and R. Lake, "Tunnel diodes," *Encyc. Appl. Phys.*, vol. 22, pp. 335–358, 1998.

[6] S. L. Rommel *et al.*, "Room temperature operation of epitaxially grown Si/SiGe/Si resonant interband tunneling diodes," *Appl. Phys. Lett.*, vol. 73, pp. 2191–2193, 1998.

[7] S. L. Rommel *et al.*, "Si-based interband tunneling devices for high-speed logic and low power memory applications," in *IEDM Tech. Dig.*, 1998, pp. 1035–1037.

[8] H. Jorke, H. Kibbel, K. Strohm, and E. Kasper, "Forward-bias characteristics of Si bipolar junctions grown by molecular beam epitaxy at low temperatures," *Appl. Phys. Lett.*, vol. 63, pp. 2408–2410, 1993.

[9] R. Duschl *et al.*, "High room temperature peak-to-valley current ratio in Si based Esaki diodes," *Electron. Lett.*, vol. 35, pp. 1111–1112, 1999.

[10] C. P. Parker *et al.*, "Temperature dependence of incorporation processed during heavy boron doping in silicon molecular beam epitaxy," *J. Appl. Phys.*, vol. 71, pp. 118–125, 1992.

[11] E. Friess, J. Nutzel, and G. Abstreiter, "Phosphorus doping in low temperature silicon molecular beam epitaxy," *Appl. Phys. Lett.*, vol. 60, pp. 2237–2239, 1992.

[12] H. J. Gossman, F. C. Unterwald, and H. S. Luftman, "Doping of Si thin films by low-temperature molecular beam epitaxy," *J. Appl. Phys.*, vol. 73, pp. 8237–8241, 1993.

[13] D. J. Eaglesham, H. J. Gossman, and M. Cerullo, "Limiting thickness h_{epi} for epitaxial growth and room-temperature Si growth on Si (100)," *Phys. Rev. Lett.*, vol. 65, pp. 1227–1230, 1990.

[14] H.-J. Gossman *et al.*, "Point defects in Si thin films grown by molecular beam epitaxy," *Appl. Phys. Lett.*, vol. 61, pp. 540–542, 1992.

[15] D. D. Perovic *et al.*, "Microvoid formation in low-temperature molecular beam epitaxy grown Si," *Phys. Rev. B*, vol. 43, pp. 14 257–14 260, 1991.

[16] G. Lippert, H. J. Osten, D. Kruger, and P. Gaworzewski, "Heavy phosphorus doping in molecular beam epitaxial grown silicon with a GaP decomposition source," *Appl. Phys. Lett.*, vol. 66, pp. 3197–3199, 1995.

[17] A. G. Chynoweth, R. A. Logan, and D. E. Thomas, "Phononassisted tunneling in silicon and germanium esaki junctions," *Phys. Rev.*, vol. 125, pp. 877–881, 1962.

[18] R. A. Logan and A. G. Chynoweth, "Effect of degenerate semiconductor band structure on current-voltage characteristics of silicon tunnel diodes," *Phys. Rev.*, vol. 131, pp. 89–95, 1963.

[19] A. G. Chynoweth, W. L. Feldman, and R. A. Logan, "Excess tunnel current in silicon Esaki junctions," *Phys. Rev.*, vol. 121, pp. 684–713, 1961.

[20] S. Sze, *Physics of Semiconductors*, 2nd ed. New York: Wiley, 1985.

[21] D. Meyerhoffer, G. A. Brown, and H. S. Sommers, "Degenerate germanium I. Tunnel, excess and thermal current in tunnel diodes," *Phys. Rev.*, vol. 26, pp. 1329–1341, 1962.

[22] S. M. Sze, *VLSI Technology*. New York: Mc-Graw-Hill, 1988, pp. 286–288.

[23] R. A. Logan, W. M. Augustyniak, and J. F. Gilbert, "Electron bombardment damage in silicon Esaki diodes," *J. Appl. Phys.*, vol. 32, pp. 1201–1205, 1961.

[24] O. Madelung, M. Schultz, and H. Weiss, Eds., *Landolt:Bornstein: Numerical Data and Functional Relationships in Science and Technology*. ser. Technology of Si, Ge, and SiC. Berlin, Germany: Springer-Verlag, 1984, vol. 17.

[25] P. Shewmon, *Diffusion in Solids*. Warrendale, PA: Minerals, Metals, Mater. Soc., 1989, pp. 19–21.

[26] R. B. Fair, "Concentration profiles of diffused dopants in silicon," in *Impurity Doping Processes in Silicon*, F. F. Y. Wang, Ed. Amsterdam, The Netherlands: North Holland, 1981, ch. 7.

[27] P. E. Thompson *et al.*, "Si resonant interband tunnel diodes grown by low-temperature molecular beam epitaxy," *Appl. Phys. Lett.*, vol. 75, pp. 1308–1310, 1999.

[28] G. G. Macfarlane, T. P. McLean, J. E. Quarrington, and V. Roberts, "Fine structure in the absorption edge spectrum of Si," *Phys. Rev.*, vol. 111, pp. 1245–1254, 1958.

Michael W. Dashiell was born in Baltimore, MD. He received the B.S. degree in electrical engineering from the University of Delaware, Newark, in 1992, where he is currently pursuing the Ph.D. degree. His dissertation focuses on the MBE growth and characterization of SiGeC alloys and tunnel diodes.His dissertation focuses on the MBE growth and characterization of SiGeC alloys and tunnel diodes.

He was with Astropower Inc. as a Research Engineer from 1992 to 1996, where his work focused on the development of lightweight GaAs solar cells for space applications. From 1995 to 1996, he was the principle investigator for SBIR programs focusing on the development of novel electrostatic-bonded solar cells. In 1996, he returned to the University of Delware to work with Prof. J. Kolodzey on SiGeC molecular beam epitaxy and devices. He will join the Max Planck Institute for Solid State Physics, Stuttgart, Germany, as a Post-Doctoral Fellow, in October 2000.

Ralph T. Troeger received the B.S. degree (Diplomingenieur) in electrical engineering from the Technical University of Chemnitz-Zwickau, Germany, in 1997, and the M.S. degree in electrical engineering from the University of Delaware, Newark, in 2000, where he is currently pursuing the Ph.D. degree in electrical engineering at the University of Delaware.

Sean L. Rommel (M'00) received both the B.S.E. and Ph.D. degrees in electrical engineering from the University of Delaware, Newark, in 1996 and 2000, respectively. His Ph.D. dissertation developed a process for the realization of Si-based tunnel diodes that could be integrated into a CMOS or SiGe HBT fabrication line.

Since June 2000, he has been a Post-Doctoral Research Associate at the University of Illinois, Urbana-Champaign. His research interests at Delaware included MSM photodetectors, optically interconnected SRAM cells, and ohmic contacts to Group IV alloys.

Dr. Rommel is the recipient of the 1997 George W. Laird Merit Fellowship and the 2000 Allan P. Colburn Prize in Engineering and Mathematical Sciences for best dissertation.

Thomas N. Adam received the B.S. degree (Diplomingeneur) in electrical engineering from the Technical University of Chemnitz-Zwickau, Germany, in 1997, and the M.S. in electrical engineering from the University of Delaware, in 2000. His M.S. work involved research on electro-optical simulation of VCSEL diodes. His doctoral research with Prof. J. Kolodzey involves the growth of novel dielectric materials, such as Al2O3 for new MOS transistors.

Paul R. Berger (S'84–M'91–SM'97) received the B.S.E. degree in engineering physics in 1985, and the M.S.E. and Ph.D. degrees in electrical engineering in 1987 and 1990, respectively, all from the University of Michigan, Ann Arbor. His Ph.D. was on MBE growth kinetics of strained III-V compound semiconductors using RHEED, MBE selective area regrowth, and the application of these to monolithically integrated optoelectronics including guided-wave detectors/modulators and pin-MODFET photoreceivers.

From 1990 to 1992, he was employed as a post-doctorate at AT&Bell Laboratories, Murray Hill, NJ, where he continued his research on opto-electronic devices and opto-electronic integration including HBT-laser phototransmitters and 10 GHz pin-MODFET photoreceiver arrays. In 1992, he joined the faculty of the University of Delaware's Electrical and Computer Engineering Department, where he was Assistant Professor from 1992 to 1997, and then became Associate Professor. His current research interests include: Si-based tunnel diodes for high-speed logic and low power memory applications; alternative organometallic precursors for MOCVD growth; conjugated polymer photonic and electronic devices and processing; and optoelectronic materials, devices and device integration.He has co-authored over 60 refereed journal articles, over 50 conference presentations, and two book sections. He received four U.S. patents, with two more patents pending on Si-based tunnel diodes and eight more on polymeric LEDs.

Dr. Berger is a member of the MRS and OSA. He has served on the Program Committee of the 1997 and 1998 IEEE International Electron Devices Meeting. Dr. Berger received the 1996 CAREER Award for Si-based Alloys and the 1998 DARPA ULTRA Sustained Excellence Award for Si-based tunnel diodes.

C. Guedj was born in Gravelines, France, in 1968. He received the M.E. and M.S. degrees in materials science and the MBA at Caen in 1992, and the Ph.D degree in electrical engineering (with highest honors) from the University of Paris XI, Orsay, in 1997.

In 1998, he was a Post-Doctoral Researcher at the University of Delaware, Newark. He co-authored several papers on SiGeC growth, characterization and modeling and received the E-MRS student award in 1995. He is currently a Physicist at the Laboratory of Micro and Nanotechnology, Paul Scherrer Institute, Switzerland.

James Kolodzey (M'74-SM'90) received the Ph.D. degree in electrical engineering from Princeton University, Princeton, NJ, in 1986, for research on SiGe alloys. He is a Professor of electrical and computer engineering at the University of Delaware, Newark.

He worked at IBM Corporation and at Cray Research. From 1986 to 1989, he was an Assistant Professor of electrical engineering at the University of Illinois,Urbana-Champaign, where he established a laboratory for high frequency device measurements at cryogenic temperatures. In 1987, he worked on molecular beam epitaxy with Dr. A. Y. Cho at AT& Bell Laboratories. In 1990, he worked on SiC and SiGeC alloys with Dr. F. Koch and Dr. R. Schwarz at the Technical University of Munich. Since 1991 he has been a Professor at the University of Delaware. In 1997, he spent nine months at the University of Paris, Orsay, investigating optoelectronic devices. His research interests include the electrical and optical properties of alloys of group IV semiconductors, and their device and circuit applications. He is presently investigating silicon germanium quantum well devices and the properties of silicon carbide alloyed with germanium.

Alan C. Seabaugh (S'78–M'79) received the Ph.D. degree in electrical engineering from the University of Virginia in 1985.

He joined Texas Instrument's Central Research Laboratory in 1986, where he developed resonant tunneling devices and integration technologies for the combination of resonant tunneling diodes with high electron mobility transistors and heterojunction bipolar transistors. In 1997, he joined Raytheon Systems Company, where he developed resonant tunneling analog-to-digital converters and Si-based tunneling devices. For the period 1979 to 1986, he worked in the Electron Device Division, National Bureau of Standards. He joined the University of Notre Dame in August 1999 as Professor in the Department of Electrical Engineering. He has authored or co-authored more than 100 papers. He holds 16 U.S. patents.

He was elected to the position of Senior Member of Technical Staff at Texas Instruments in 1991, Distinguished Member of Technical Staff in 1997, and was promoted to the position of Senior Fellow at Raytheon Systems Company in 1999. He is a Member of the American Physical Society.

R. Lake received the B.S.E.E, M.S.E.E., and Ph.D. degrees from Purdue University, West Lafayette, IN, in 1986, 1988, and 1992, respectively.

He joined the Nanoelectronics Branch, Central Research Laboratories, Texas Instruments, in 1993. While at Texas Instruments, he developed the theory that drives the Nanoelectronic Engineering Modeling Tool (NEMO). His research interests include computational electronic device physics and modeling from the atomistic through the circuit level.